

## 1. Activity Mode of the 1980 Earthquake Swarm Off the East Coast of the Izu Peninsula.

By Masaru TSUJIURA,

Earthquake Research Institute.

(Received February 28, 1981)

### Abstract

An earthquake swarm activity which occurred in an area off the east coast of the Izu Peninsula during the period from June 24 to July 28, 1980 was studied on the basis of the waveform analysis. This swarm contained many bursts of activity usually lasting for about one hour. The earthquakes which occurred within a certain time interval, e.g. about 15 minutes, exhibit similar waveforms, suggesting that they belong to one "earthquake family". The epicenters of earthquakes in a family are located within a spatial dimension of a few hundred meters with the same mechanism. When the activity of the first family is finished, the second family appears in an adjacent area separated by 1.5 km at most. Four families are usually observed for the activity of about one hour, except for the activity triggered by the  $M$ 6.7 earthquake. The earthquakes in a given family distribute over the magnitude range from 2.0 to 4.9. The corner frequency of the source spectrum in a given family is almost constant within a range of 15 per cent, and its value depends on the size of the largest earthquake in a family. The largest earthquake usually occurs in the later stage of its sequence. Continuous monitoring of the spectrum therefore will give us some information useful for the prediction of the size of largest earthquake in an earthquake family.

### Introduction

The study of earthquake swarm is important not only for a better understanding the mechanism of earthquake occurrence, but also for the discrimination of the foreshock activity preceding a large earthquake from the swarm activity. In some cases, special spectral features of earthquakes were found for the swarm activity of certain regions. One of the most striking features of the swarm activity was that the earthquakes generated in a certain time interval have similar waveforms (TSUJIURA, 1979a, 1980a), which differ clearly from those of the

foreshock and normal (background) seismic activities (TSUJIURA, 1979b, 1980a).

Recently, a remarkable swarm activity was generated off the east coast of the Izu Peninsula. This activity continued for about one month. The swarm activity in this area occurred repeatedly after 1978, and the present swarm showed the highest activity (e. g., KARAKAMA *et al.*, 1980). In order to check the results obtained in our previous studies, we first studied the similarity of waveform, using the seismogram recorded at high paper speed, and later we conducted a spectral analysis using the data of narrow band-pass filters operating routinely (TSUJIURA, 1978a). We shall show some spectral features of seismic waves closely relating to its activity mode.

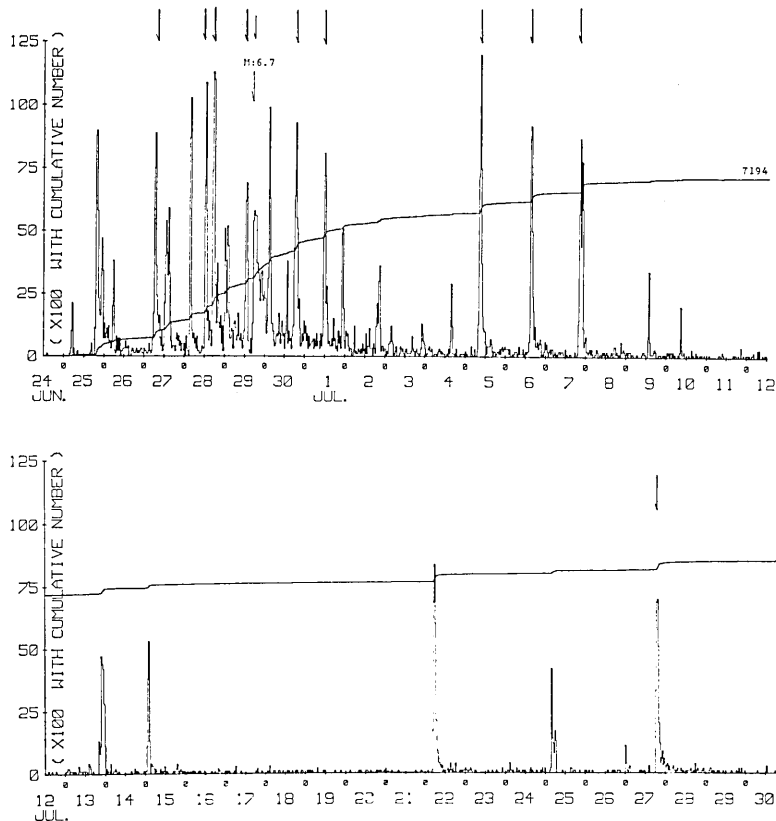


Fig. 1. Frequency distribution of the earthquakes for every 30 minutes obtained at OYM, epicentral distance being about 55 km (after ERI, 1981).

## Data

Since June 24 of 1980, many earthquakes occurred in an area off the east coast of the Izu Peninsula. This swarm continued for about one month, repeating intermittent bursts of activity. Figure 1 shows the frequency distribution of the earthquakes for every 30 minutes compiled by the Earthquake Research Institute (ERI, 1981). Figure 2 shows the records of three periods obtained at Dodaira seismic station (DDR), the epicentral distance of about 120 km. It is seen that the earthquakes are concentrated to some brief time intervals (e. g., one hour). Such continual occurrence of the earthquakes may affect the accuracy of the determination of their epicenters. As shown later, the analysis of the waveform by the superposition (overlapping) of the separated seismograms at high paper speed, however, give us more accurate information relating to its activity mode, such as the distribution of epicenters and the migration of epicenters with time (TSUJIURA, 1979a, 1980a).

Figure 3 shows the distribution of the seismic stations used in this study together with the epicentral area of the earthquake swarm determined by KARAKAMA *et al.* (1980). All seismic signals are telemetered at the ERI by the radio-waves or the telephone-line. Two different sets

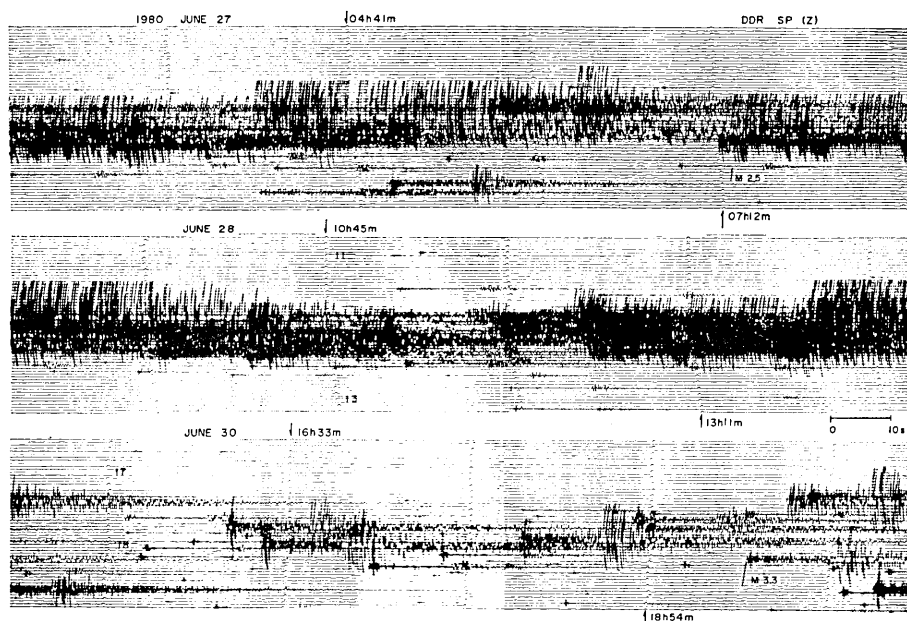


Fig. 2. Seismograms for three periods with concentrated activity obtained at DDR, epicentral distance being about 120 km.

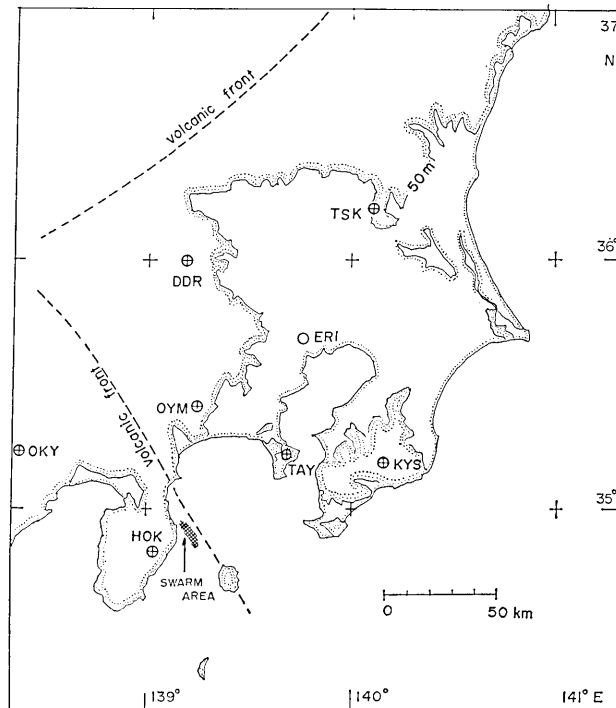


Fig. 3. Distribution of the seismic stations used in this study and the epicentral area of the earthquake swarm taken from the lists of KARAKAMA *et al.* (1980).

of data are available for the present study. One is the data recorded at high paper speed by a trigger mode with memory (TRG), and the other is the data passing through band-pass filters (BPF). Detailed description of both systems are given in a previous paper of this series (TSUJIURA, 1979a). The paper speed for TRG seismogram is adjusted to be 25 mm/sec in order to see the detailed waveforms. About 1200 earthquakes with magnitude ranging from 1.5 to 4.9 are obtained through the swarm sequence. Moreover, the DDR station has various kinds of seismographs which cover the wide-frequency band and wide-dynamic range, and their seismograms are recorded continuously on a magnetic tape (TSUJIURA, 1973). These seismograms are also usable for the analysis of large events ( $M > 3.2$ ).

We are especially interested to know the activity mode in the most active stage of the swarm. The 10 sequences indicated by arrows in Figure 1 are finally selected, and the analysis of waveform is made by superimposing the TRG seismograms.

## Similarity of waveform

In the course of examining the waveform by the superposition of the TRG seismograms, it was found that the seismograms obtained in a brief time interval (e. g., 15 minutes) exhibit similar waveforms independent of earthquake size. Figure 4 shows an arrangement of seismograms obtained at HOK during the 15 minute interval from 02h 33m to 02h 48m, June 28. High correlation of the waveforms are clearly seen between the corresponding traces, including *P*, *S* and several isolated

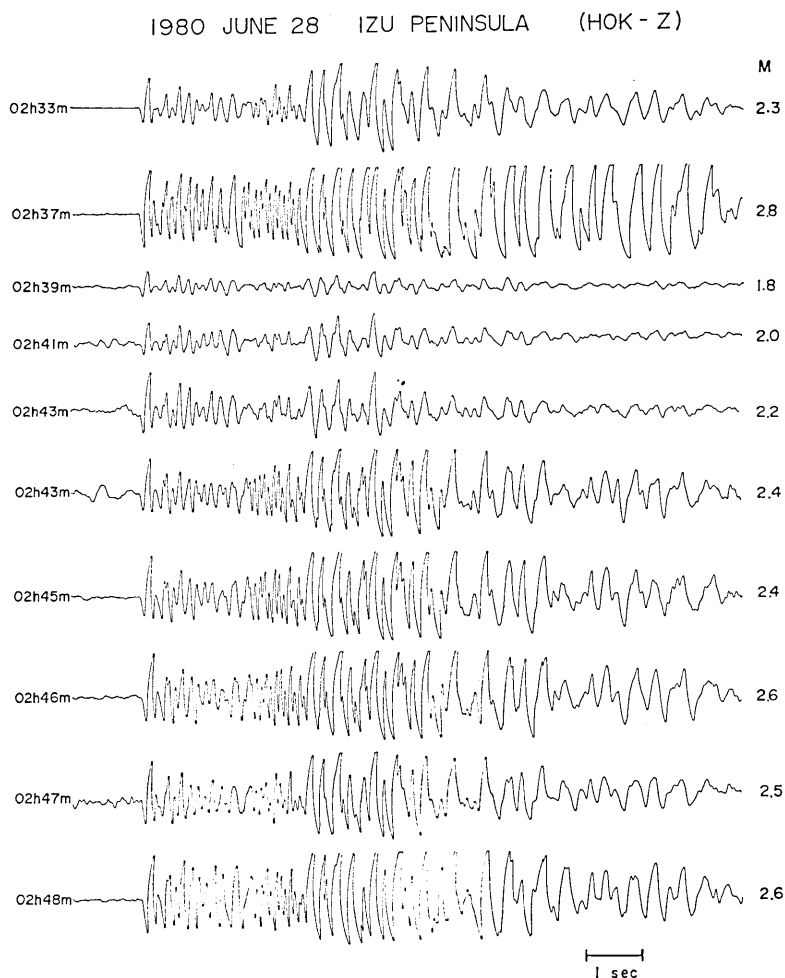


Fig. 4. An arrangement of the seismograms obtained by the vertical component (*Z*) at HOK during a period of 15 minutes. Magnitudes of these events lie between 1.8 and 2.8. Note the high correlation of the corresponding traces between the seismograms.

waves. Especially, when the seismograms with similar size are compared, their waveforms coincide almost perfectly from *P*-wave onset till coda waves. The events with similar waveforms, of course, will be expected to have similar *S-P* times. In fact, we found that the deviation of *S-P* times of their seismograms falls within a range of 0.06 sec.

The similarity of the waveforms can be expected in the seismograms of the other stations. Figure 5 shows an example of the seismograms of the event pair obtained at five stations distributed around the swarm

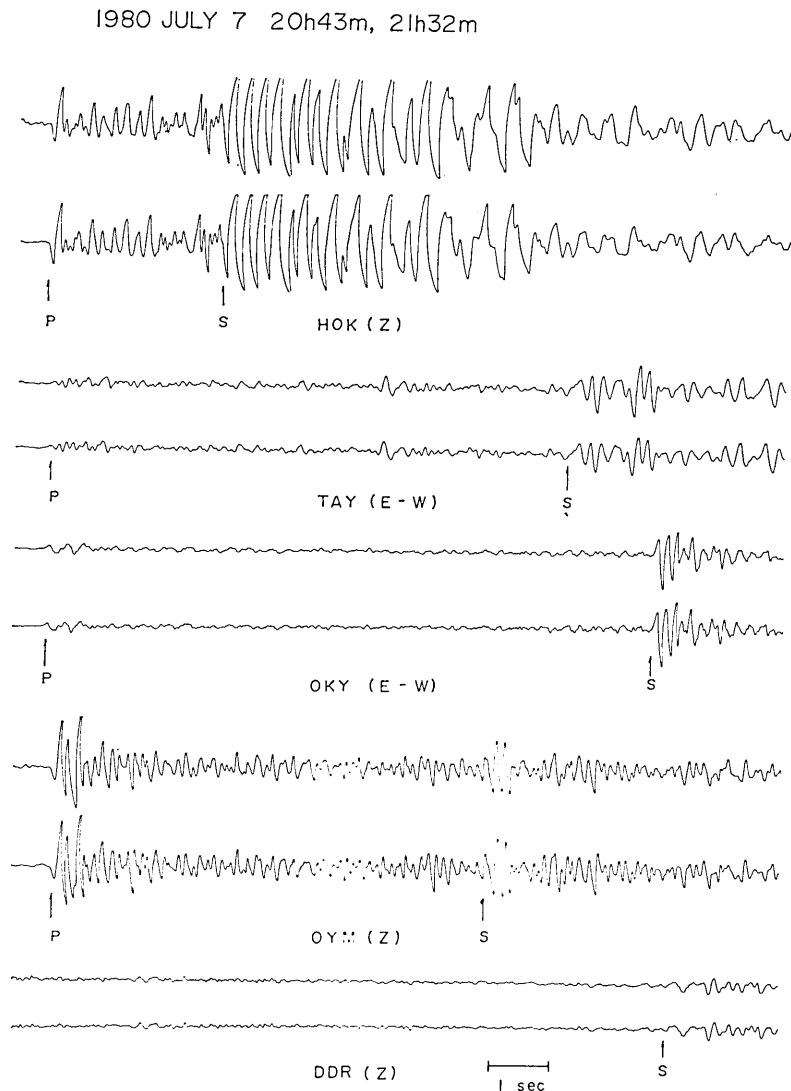


Fig. 5. An example of the seismograms for the event pair with almost exact agreement of the waveform and *S-P* time at each station.

area. The close similarity of waveforms is clearly found between the event pair at each station, and the  $S$ - $P$  time at each station also does not differ no more than by 0.05 sec. According to our previous study, such a behavior suggests that their earthquakes are distributed within a spatial dimension of about 400 meters with almost the same mechanism (TSUJIURA, 1980a). Thus we may conclude that earthquakes occurring during a certain short time interval in the 1980 earthquake swarm have very similar waveforms. The same conclusion was obtained in our previous studies of different earthquake swarms. We call hereafter these earthquakes with similar waveforms a group of similar earthquake or an "earthquake family" (HAMAGUCHI and HASEGAWA, 1975).

### Recurrent occurrence of earthquake family

The time interval between two successive earthquake families depends on the degree of seismic activity. When the seismic activity is high, the time interval is short and another family appears soon after the activity of the initial family is finished. Figure 6 shows an example of the seismograms of two families separated at the time of 01h 27m. The similarity of waveforms and the equality of  $S$ - $P$  times are recognized clearly for each family, and the dissimilarity of the waveforms between two families is also noticed clearly in the  $P$ -wave portion where the polarity of the initial motion systematically changes from compression before 01h 27m to dilatation after that time. Moreover, the  $S$ - $P$  time also changes. We found a change of about 0.1 sec by the superposition of the seismograms.

Further measurement of  $S$ - $P$  times at four stations gives the difference of the epicenters of two families. The epicenters determined using these values show that the earthquakes of the second family occurred about 1 km northwest of the first family. Figure 7 shows the temporal distribution of earthquakes in the two families shown in the previous figure. The amplitude of each event shows the relative amplitude of  $S$ -wave in 3 Hz band taken from the filtered-seismograms at DDR and TSK, and the scale of the ordinate on the right-hand side indicates the magnitude ( $M$ ) determined by the  $F$ - $P$  time method at DDR given by HORI (1973). Solid and dashed lines represent the upward and downward initial motions at HOK, respectively. It is interesting that there is a systematic difference in the polarity of initial motion between the earthquake families as was previously mentioned. The polarity of initial motion at the other stations, however, does not change. Consider-

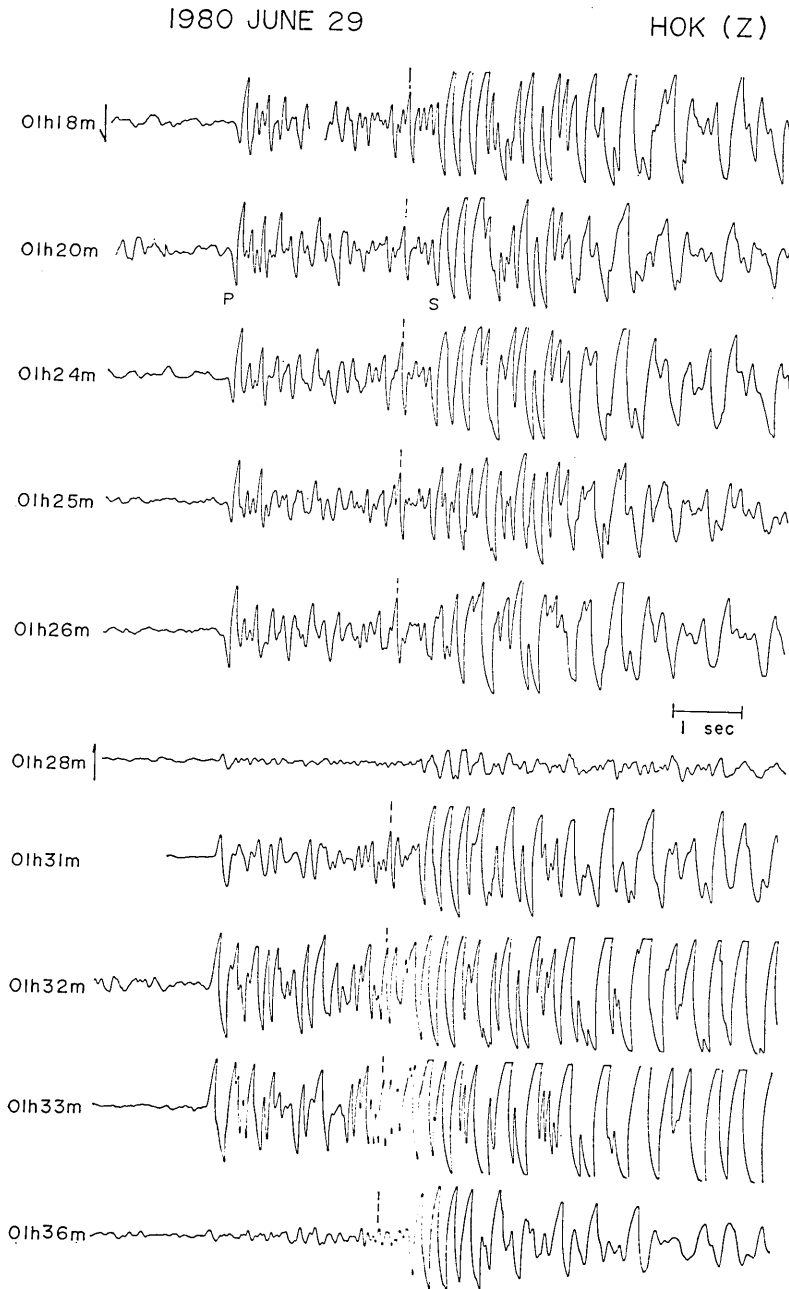


Fig. 6. An example of the seismograms for two earthquake families separated by 01 h 27 m. Note the difference of the polarity of initial motion of *P*-waves between two families.



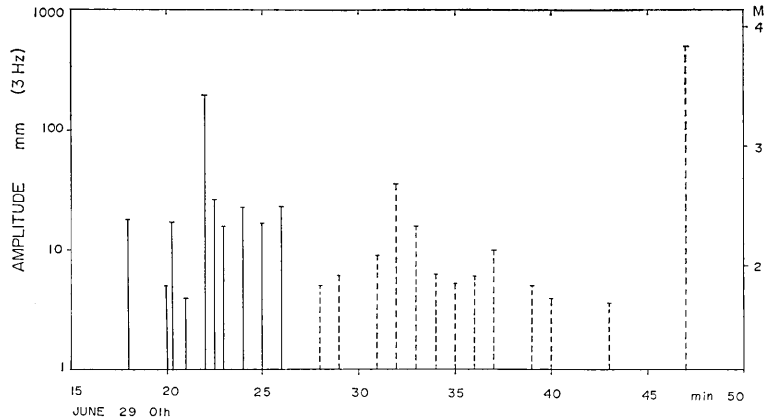


Fig. 7. Distribution of the earthquakes belonging to two earthquake families. Solid and dashed lines show the upward and downward initial motions at HOK, respectively. The amplitude and magnitude ( $M$ ) are determined on the basis of the filtered-seismograms at DDR and TSK.

ing the station arrangement of our network, it is expected that the difference of the source mechanism between two families is not large. There may be only a slight change in the dip and strike of the nodal planes, and the station HOK probably lies near the nodal planes.

Figure 8 shows an example of the distribution of earthquake families during a 70-minute period of concentrated activity. Numerals at the top show the group number of earthquake family. We find that during a

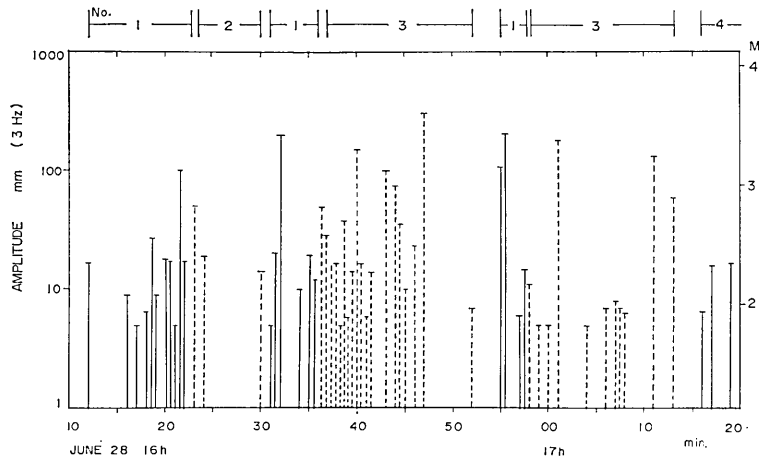


Fig. 8. Distribution of earthquake families obtained for a swarm sequence of 70-minutes with concentrated activity. Numerals indicated in the upper abscissa is the group number of the earthquake family. Explanation of the other symbols is the same as those of Fig. 7.

certain active period several earthquake families of different source mechanism appear alternately. For example, the earthquake family represented by solid lines (No. 1) appears at first, and its activity continues for about 10 minutes. After the activity of the first family stopped, the second family represented by dashed lines starts. When the No. 2 family finished, the No. 1 family again appears, and similar activities repeat until its sequence is finished. The  $S-P$  times for events in each family do not differ by more than about 0.06 sec, and the  $S-P$  times for events in the different families may differ by about 0.2 sec. Such evidence suggests that the earthquakes in the active period do not occur randomly in space. They occur only within several limited small areas.

Figures 9 and 10 show the activity mode of earthquakes in other sequences. Alternate occurrence of four families is apparent. Two large earthquakes with  $M \geq 4.5$  occurred in each sequence. Such events are usually followed by aftershocks. In the present case, however, the activity preceding the  $M4.5$  earthquake is higher than the activity following the event. This is probably one of the most important features of the activity of similar earthquakes. This feature can qualitatively be explained as follows. The earthquakes belonging to a family occur on the same fault plane as repeated slipping, and the largest event with  $M4.5$

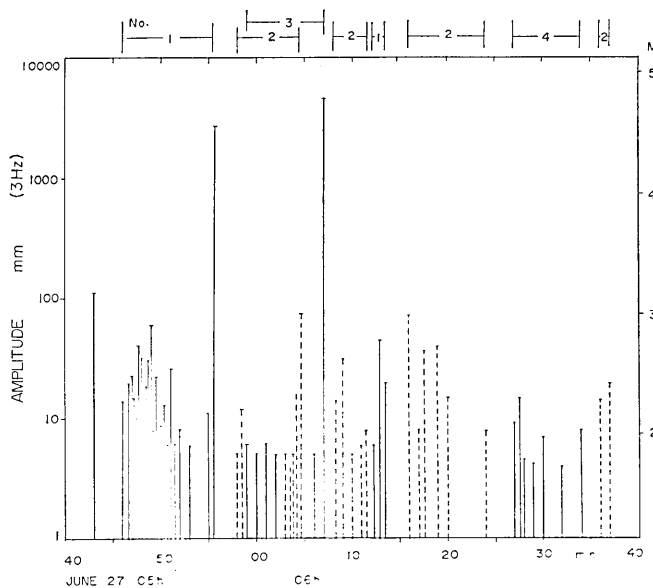


Fig. 9. Distribution of the earthquake families including large events with  $M \geq 4.5$ . Note that the activity preceding the large earthquake is more dominant than the activity following the event. Explanation of the other symbols is the same as those of Fig. 7.

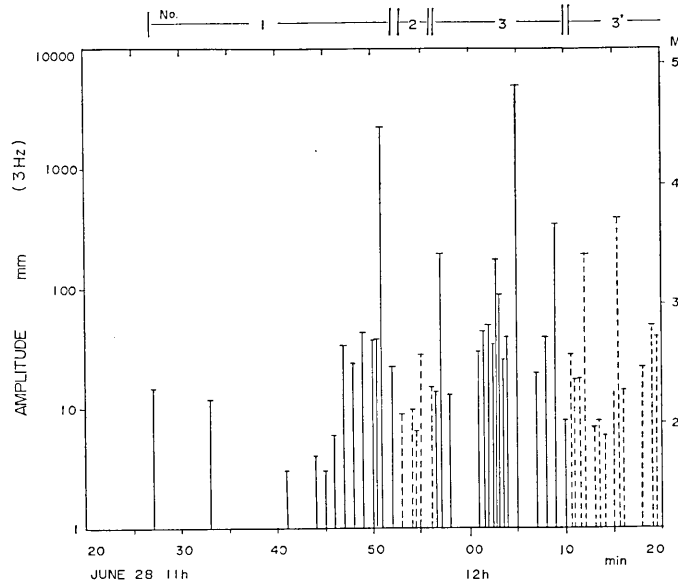


Fig. 10. Distribution of earthquake families including the large events with  $M \geq 4.5$ .

occurs as the earthquake with the maximum slip or complete rupture corresponding to the "highest stress drop earthquake" (AKI *et al.*, 1977). Consequently, only a weak activity will be followed on the same fault plane. On the other hand, this maximum stress release produces the stress concentration elsewhere, and promotes the occurrence of another family.

Figure 11 shows the distribution of earthquake families in a sequence belonging to the later stage of the 1980 swarm. There is no systematic variation of the polarity of initial motion. The activity still consists of four families with their own waveform features.

We studied the activity mode for ten sequences, each of which lasts about one hour. Table 1 shows the proportion of earthquakes occurring in families together with the number of families recognized. We found that about 80 per cent of the earthquakes belong to the earthquake families.

Besides the earthquake groups described above, the activity associated with a specially large earthquake with  $M=6.7$  occurring on June 29 must be noted. The activity mode of the sequence including the  $M6.7$  earthquake is quite different from the other sequences. For example, the  $M6.7$  shock appeared suddenly without any preceding small earthquake and was followed by many small earthquakes. This suggests the activity

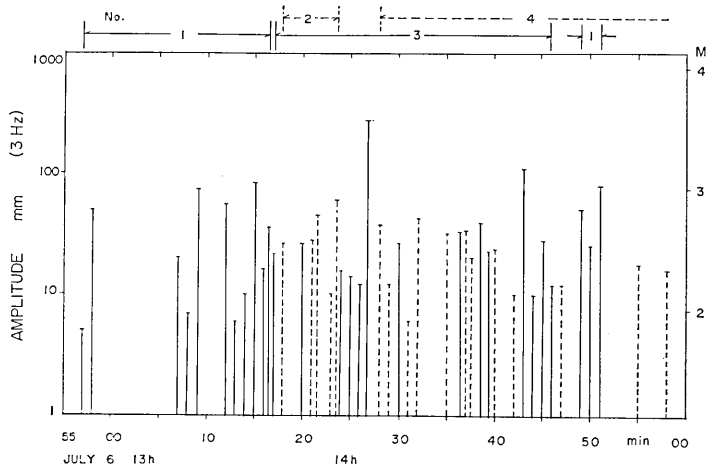


Fig. 11. Distribution of earthquake families obtained for the activity belonging to the later stage of the swarm sequence.

Table 1. Ratio of the number of earthquakes belonging to earthquake families to the total number of earthquakes.  $N$ ; total number of earthquakes concerned,  $n$ ; number of earthquakes in the family,  $F$ ; number of earthquake families,  $M_{\max}$ ; magnitude of the largest earthquake included in each family.

Date	Time				$N$	$n$	$n/N$ %	$F$	$M_{\max}$
	h	m	h	m					
June 27	05	43	06	37	77	65	84	4	4.9
June 28	11	25	12	20	80	66	83	4	4.9
June 28	16	12	17	19	87	70	80	4	3.8
June 29	12	07	13	12	44	35	80	4	3.2
June 30	17	20	18	15	56	41	73	5	3.6
July 1	10	45	11	40	50	40	80	5	3.4
July 5	07	45	09	02	51	38	75	6	3.3
July 6	13	58	14	58	77	61	79	4	4.1
July 7	19	43	20	57	42	34	81	4	4.5
July 27	17	49	18	50	53	35	66	4	4.6

of the main shock-aftershock type. The activity mode for 41 earthquakes which occurred during three hours after the  $M6.7$  earthquake is studied by the same procedure. All of these events appear with an individual waveform character except for two event pairs with similar waveforms, and no earthquake family was observed.

Detailed study of the activity mode including the migration of epicenters with time is very useful for better understanding of the mechanism of the earthquake swarm. We studied here the distribution of  $S-P$

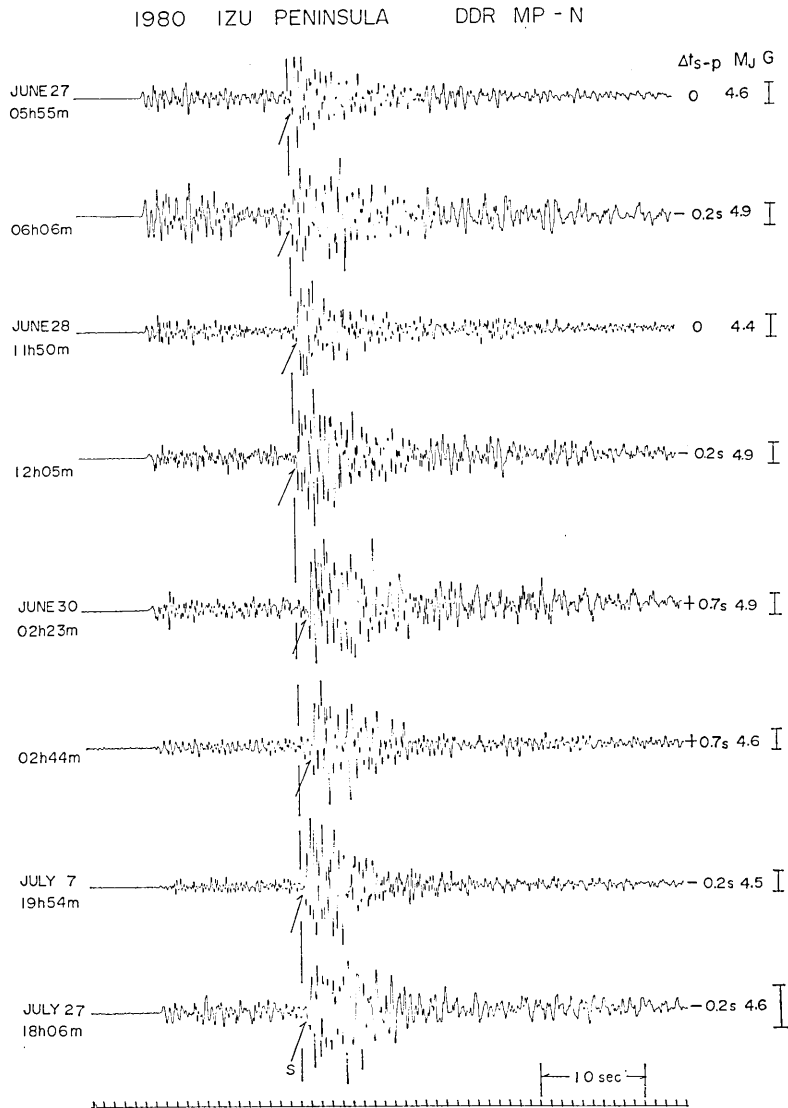


Fig. 12. Seismograms of major events ( $M_J \geq 4.4$ ) in the whole swarm sequence obtained by the medium-period seismograph (MP) at DDR.  $\Delta t_{s-p}$ ; relative difference of the  $S-P$  time against the reference earthquake (top seismogram),  $M_J$ ; magnitude determined by the Japan Meteorological Agency, G; relative difference of the gain of play-back amplifier.

times for major events with  $M \geq 4.5$  which are the largest event in each family. Figure 12 shows the seismograms obtained by the medium-period seismograph (MP) at DDR. The magnitude determined by the Japan Meteorological Agency (JMA) is shown at the end of each seismogram by  $M_J$ . Except for the event with  $M 6.7$ , eight events with  $M_J \geq 4.4$  were obtained throughout the swarm sequence. The difference in  $S$ - $P$  times from the reference earthquake (top seismogram) is also shown at the end of each seismogram by  $\Delta t_{S-P}$ . We found that the difference in  $S$ - $P$  times falls within a range of 0.9 sec. In particular, the difference of  $S$ - $P$  time for the event pairs which occurred during a time interval of about 20 minutes lies within a range of 0.2 sec. Similar measurement of  $S$ - $P$  time for the same events using the MP seismograms at KYS gives much smaller deviation of about 0.6 sec. The station DDR is located roughly to the north of the swarm area. The epicenters determined by KARAKAMA *et al.* (1980) throughout the sequence show a linear focal zone orientated roughly north-south with a length of about 20 km. However, if we consider the distribution of  $S$ - $P$  times for major earthquakes, their epicenters do not spread as much as those obtained by the other study. In other words, our estimation suggests that major earthquake swarms concentrate within an area of about 7 km if we assume the Omori constant of 8 km/sec.

### Spectral analysis

In order to obtain the source parameters of the earthquake swarm the spectral analysis is made for  $S$ -waves using the records of band-pass filters operating routinely at three stations. The filtered records of nine earthquakes belonging to the same family, obtained during about 20 minutes are shown in Figure 13. The method of analysis is the same as that in our previous studies (e. g., TSUJIURA, 1978a). The maximum amplitudes of  $S$ -waves ( $A_S$ ) are measured directly on the six-band filtered traces. Following AKI and CHOUET (1975), the spectral density from the records of band-pass filters is given as

$$A_S = 2\Delta f |F(\omega)|$$

where  $F(\omega)$  is the spectral density and  $\Delta f$  is the bandwidth for a given channel. From the known bandwidth of the band-pass filter and the maximum amplitude of  $S$ -waves measured on each frequency, the amplitude spectral density is estimated. However, as pointed out by RAUTIAN and KHALTURIN (1978), and AKI (1980), the above equation may not apply in the case of non-impulsive waveform. In our seismograms,  $S$ -waves

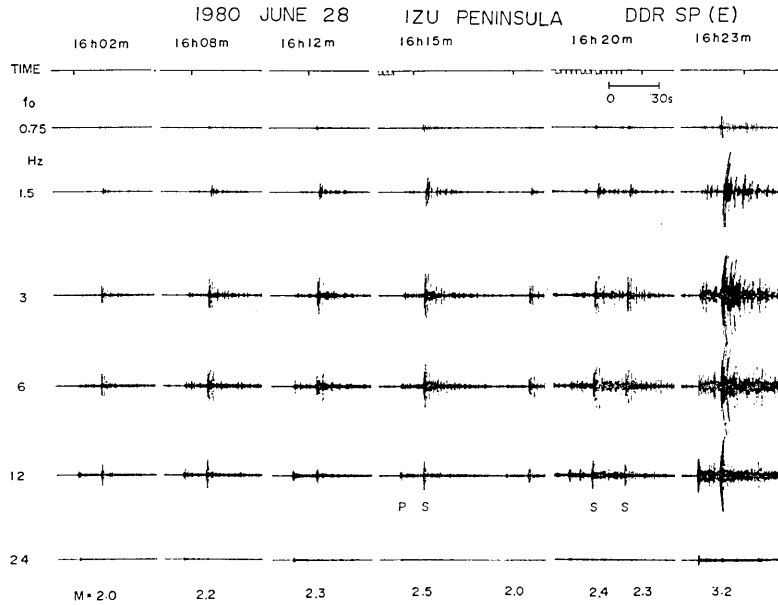


Fig. 13. Examples of the filtered-seismograms for an earthquake family.  $f_0$ ; center frequency of the band-pass filter.

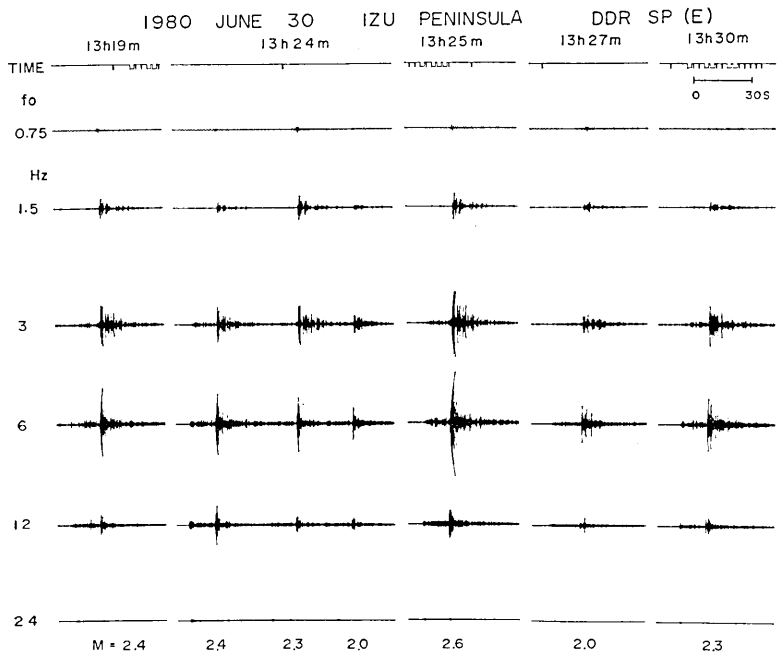


Fig. 14. Examples of the filtered-seismograms. Note the difference of the amplitude ratio of 6 Hz/3 Hz from those shown in Fig. 13.

for two channels centered at 3 and 6 Hz show non-impulsive waveforms, which continue for a few cycles with comparable amplitudes. The  $|F(\omega)|$  of these channels therefore will give an underestimation by a factor roughly equal to the square root of the number of cycles in the wave train (AKI, 1980). Despite of these uncertain seismograms, we found clear differences in the spectrum between the earthquake families. Figure 14 shows the filtered seismograms belonging to another family. The amplitude ratio for 6 and 3 Hz bands of these seismograms is large at least by a factor of two compared with those shown in Figure 13.

Using these seismograms, we obtained the source spectrum correcting for the effect of attenuation along the propagation path and the local site effect at the seismic station (TSUJIURA, 1979a). The source spectra obtained from the earthquakes belonging to two families are shown in Figure 15. Since our data are the output of band-pass filters, the low-

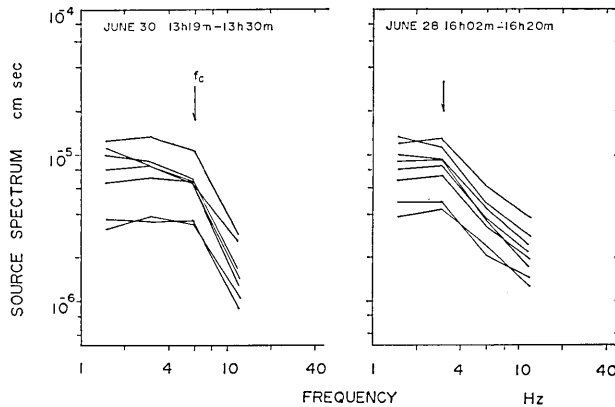


Fig. 15. Comparison of the source spectra of earthquakes belonging to two earthquake families.

frequency spectral level ( $\Omega_0$ ) and the corner frequency ( $f_c$ ) are approximated by fitting two straight lines that intersect at the corner frequency to the observed spectra. The approximate corner frequency is indicated by arrows. The corner frequency of events in a given family shows more or less the same value, independent of the absolute values of amplitudes, with minor differences in the shape of high frequency component. Such a behavior is consistent with the results of other swarm activities (TSUJIURA, 1979a, 1980a). Figure 16 shows the source spectra of another group of families. Each family consist of the earthquakes preceding a large earthquake with  $M_j \geq 4.4$ . The corner frequency of these groups is about 3 Hz.



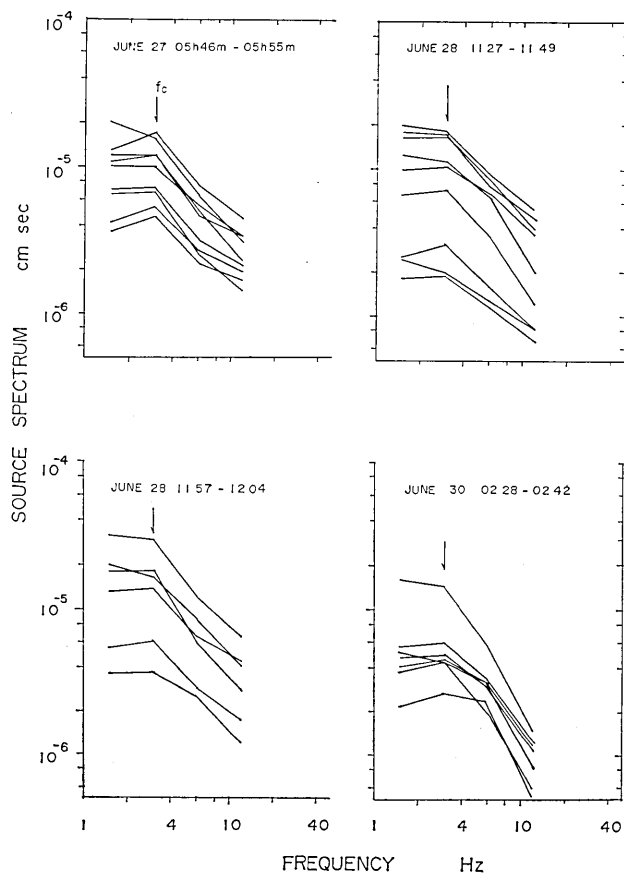


Fig. 16. Source spectra of small earthquakes preceding the large earthquake with  $M_J \geq 4.4$ .

As discussed earlier, the amplitudes for a frequency band between 3 and 6 Hz give an underestimation. Considering the uncertainty of the seismograms shown in Figure 13, the spectral level of these frequencies gives an underestimation roughly by a factor of 0.5. The corner frequency therefore may be overestimated. Even considered the uncertainty of our estimation, there exists a clear difference in the source spectrum between the families, which can be attributed to the difference of corner frequency. The corner frequency obtained here lies between 3 and 6 Hz. Some events with corner frequency of about 1.5 Hz can be seen after the main event of  $M=6.7$ . Such events, however, did not belong to any earthquake family. Table 2 shows the distribution of the corner frequency of earthquakes with  $M \approx 2.5$  for 12 families. The magnitude of the largest earthquake included in each family is also shown for the

Table 2. Distribution of the corner frequency ( $f_c$ ) of earthquakes with  $M \approx 2.5$  for 12 earthquake families.  $M_{\max}$ ; magnitude of the largest earthquake included in each family. The time indicated by bracket shows the occurrence time of the largest earthquake.

Date	Time				$f_c$ Hz	$M_{\max}$	(Time)	
	h	m	h	m			h	m
June 25	21	50	— 22	40	5	2.9	22	00
June 27	05	43	— 06	14	3	4.9	06	06
June 28	02	33	— 03	00	4.5	3.5	03	00
June 28	11	47	— 12	20	3	4.9	12	05
June 28	16	02	— 16	47	3	3.8	16	47
June 29	01	18	— 01	27	3	3.7	01	22
June 29	12	08	— 12	31	6	3.1	12	24
June 30	13	13	— 13	30	6	2.9	13	20
June 30	18	15	— 18	36	6	3.2	18	36
July 2	18	48	— 20	30	6	3.0	19	53
July 5	07	58	— 08	55	6	3.3	08	25
July 6	14	07	— 14	35	3	4.1	14	19

comparison. It is interesting that there is some correlation between the corner frequency and the size of the largest event. The family with low corner frequency, on the average, contains larger event comparing with that of high corner frequency. Further discussion of this problem will be given by a separate paper.

### Source spectrum of earthquake family

As described in the preceding section, the earthquakes in a given family are distributed over a magnitude range from 2.0 to 4.9. In order to know spectral features of the whole earthquake family, seismograms of the medium-period seismograph (MP) recorded on a magnetic tape are used for large event ( $M \geq 3.2$ ) because our short-period seismograph has a limited dynamic range. The spectral analysis using the band-pass filters with 1/3 octave bandwidth is made for large events included within the family. Figure 17 shows the source spectra of large events together with the source spectra of small events obtained earlier (dashed lines). From the combined data of small and large events, we now constructed a scaling law of the source spectrum of earthquake family. Although the high frequency asymptote shows a steeper slope for  $M, 4.6$  than for  $M, 3.2$ , the corner frequency is nearly constant over the magnitude range from 2.0 to 4.6. Such behavior is quite different from those expected from the ordinary scaling law of seismic spectrum (AKI, 1967,

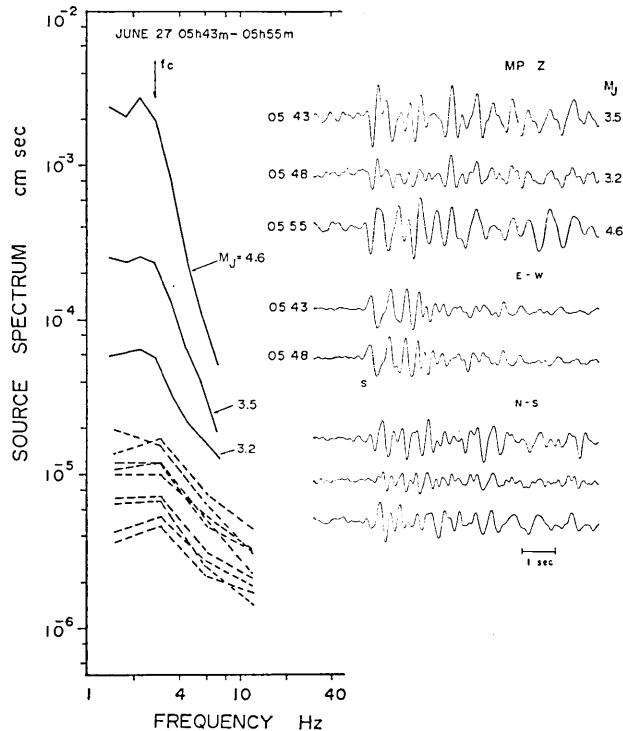


Fig. 17. Source spectra of earthquakes belonging to an earthquake family. Top spectrum corresponds to the  $M_J=4.6$  earthquake.

1972), and the relation between the period of initial motion and magnitude of earthquakes (TERASHIMA, 1968). This disagreement may be partly due to the difference in the source process. The earthquakes belonging to the given family occur over the same fault plane bounded by barriers, and the difference of the earthquake size may be caused by the difference of the average slip length over the fault plane (TSUJIURA, 1979a). The path of constant corner frequency and the difference of the steepness of high frequencies can be explained also by a model of rupture propagation in a heterogeneous medium proposed by DAS (1976).

Using the circular crack model of MADARIAGA (1976), who gives the relation of  $f_c=0.21 \beta/a$ , we estimate the fault radius ( $a$ ) corresponding to the corner frequency ( $f_c$ ), assuming  $\beta=3.5$  km/sec. We found a radius of 250 meters if we take 2.8 Hz corner frequency. Considering the source size and the epicentral area, it is expected that they are occurring along the same fault plane as repeated slipping.

From each flat low frequency level ( $\Omega_0$ ), the corresponding seismic moment ( $M_0$ ) is determined by using Brune's model (BRUNE, 1970), assum-

ing the values adopted by TSUJIURA (1979a). The result shows the average seismic moment of  $1 \times 10^{20}$  dyne cm for  $M=2.0$  and  $5 \times 10^{22}$  dyne cm for  $M=4.6$  earthquakes, respectively. Using  $M_0$  and  $a$  obtained above, the value of stress drop ( $\Delta\sigma$ ) is estimated by using Brune's model. The stress drop obtained here shows the values of 3.5 bars for  $M2.0$  and 650 bars for  $M4.6$  earthquakes, respectively. It is noticed that the stress drop obtained using a radius of Madariaga's formula is about six times greater than that using Brune's formula. Even considering the difference of our estimation the stress drop of  $M4.6$  earthquake shows greater value than those estimated earlier (THATCHER and HANKS, 1973; ISHIDA, 1974; JOHNSON and MCEVILLY, 1974; TSUJIURA, 1978b). Thus, we may conclude that the earthquake of  $M4.6$  occurred as the earthquake with maximum slip corresponds to the maximum stress drop earthquake in a given fault. Because of the large stress drop, all the stress may be released and no more aftershocks follow.

### Discussion and conclusion

From the analysis of waveform and spectrum, we found the salient features of the earthquake swarm activity. The earthquake activity in a certain short time interval (e. g., 15 minutes) consists of events with similar waveforms belonging to an earthquake family. The epicenters of earthquakes in a family cluster in a domain with a linear dimension of a few hundred meters, suggesting that they occur on the same fault plane bounded by barriers.

When the activity of the first family is finished, the second family starts in an adjacent area separated by 1.5 km at most, and similar activities are repeated until its sequence is finished. Four families are usually observed over a sequence of about one hour. Such evidence suggests that the earthquakes in a given time interval did not occur randomly in space, they occurred only on the specified faults distributed within an area of about 2 km. A similar activity mode was observed for ten sequences with concentrated activity.

A large earthquake with  $M=6.7$  was observed about five days after the beginning of the swarm. The activity mode for the  $M6.7$  earthquake and its followers is quite different from those of the other activities. They showed the activity of the main shock-aftershock type, and no earthquake family was observed. There are some argument on whether the seismic activities preceding the  $M6.7$  earthquake are the foreshocks or the earthquake swarm. Considering the difference of activity mode

between the two activities, we may conclude that they are the earthquake swarm, because they show regular activity mode which differs from that of foreshock activity (TSUJIURA, 1979b). The earthquake swarm usually does not include specially large earthquake (MOGI, 1963). Our study of the earthquake swarm in the Kanto district is consistent with Mogi's result except for the 1978 earthquake swarm in the same area (TSUJIURA, 1980b). Thus, it may be suggested that the occurrence of an especially large earthquake during a swarm may depend on the tectonic nature of the swarm area.

Through the swarm sequence, eight events with magnitudes around 4.6 were observed, but never found the event above  $M5.0$  except for the  $M6.7$  event with a different activity mode. The reason for the absence of large earthquake may partly be due to the limited available stress drop. Our observation of the corner frequencies of an earthquake family indicates that they are nearly constant within a range of 2.6 and 3 Hz for magnitudes between 2.0 and 4.6. This evidence suggest that the stress drops of the events belonging to an earthquake family is proportional to the earthquake size. Our estimation of the stress drop shows a value of about 650 bars for the  $M4.6$  earthquake. If there occurs an event with  $M5$ , the stress drop may exceed 1 kbars. Such a value will be too large

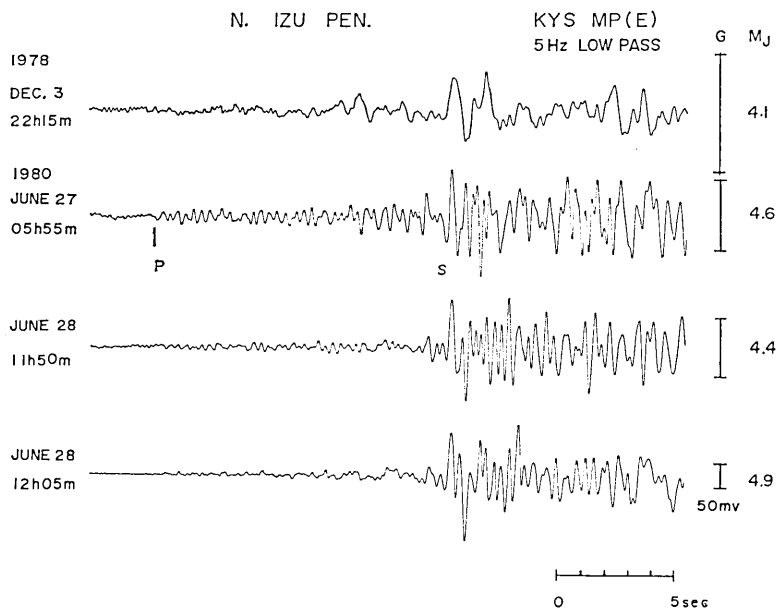


Fig. 18. Comparison of the seismograms for two swarm sequences. Note that low-frequency waves predominate in the 1978 seismogram. G; relative difference of the gain of play-back amplifier.

for the stress drop of  $M_5$  earthquake, and different corner frequency will be needed. In fact, we found the seismograms supporting the above conclusion. Figure 18 shows the comparison of the seismograms of two swarm sequences. One is the largest event in each family taken from the present swarm and the other is the event preceding the main event of  $M_J=5.4$  which occurred on December 3, 1978 in the same area. The seismogram of Dec. 3 shows remarkably low frequency waves in spite of its smaller magnitude. The largest event in a given family occurs in its later stage (TSUJIURA, 1980b). Thus, we may conclude that the corner frequency of the former events gives some information useful for the prediction of the size of largest event. If such features are commonly observed for other swarm sequences, continuous monitoring of the seismic spectrum may be useful for the prediction of the largest earthquake in a given swarm sequence.

#### Acknowledgment

I am grateful to Prof. Keiiti Aki of Massachusetts Institute of Technology and Prof. Tokuji Utsu of Earthquake Research Institute, University of Tokyo, who read the manuscript critically and offered many valuable suggestions.

#### References

- AKI, K., 1967, Scaling law of seismic spectrum, *J. Geophys. Res.*, **72**, 1217-1231.
- AKI, K., 1972, Scaling law of earthquake source time-function, *Geophys. J. Roy. Astron. Soc.*, **31**, 3-35.
- AKI, K., 1980, Scattering and attenuation of shear waves in the lithosphere, *J. Geophys. Res.*, **85**, 6496-6504.
- AKI, K. and B. CHOUET, 1975, Origin of coda waves: source, attenuation, and scattering effect, *J. Geophys. Res.*, **80**, 3322-3342.
- AKI, K., M., BOUCHON, B. CHOUET and S. DAS, 1977, Quantitative prediction of strong motion for a potential earthquake fault, *Annali di Geofisica*, **15**, 341-368.
- BRUNE, J. N., 1970, Tectonic stress and the spectra of seismic shear waves from earthquakes, *J. Geophys. Res.*, **75**, 4997-5009.
- DAS, S., 1976, A numerical study of rupture propagation and earthquake source mechanism, *Ph. D. Thesis*, Massachusetts Inst. of Technol., Cambridge.
- ERI, Earthquake Research Institute, 1981, Seismic activities in the Izu Peninsula and its Vicinity (May-October 1980), *Rep. Coordin. Commit. Earthq. Predic.*, **25**, 162-168 (in Japanese).
- HAMAGUCHI, H. and A. HASEGAWA, 1975, Recurrent occurrence of the earthquake with similar wave forms and its related problems, *Zisin*, **2**, **28**, 153-169 (in Japanese).
- HORI, M., 1973, Determination of earthquake magnitude of the local and near earthquake by the Dodaira Microearthquake Observatory, *Speci. Bull. Earthq. Res. Inst.*, **10**(4), 1-4 (in Japanese).
- ISHIDA, M., 1974, Determination of fault parameters of small earthquakes in the Kii

- Peninsula, *J. Phys. Earth*, **22**, 177-212.
- JOHNSON, L.R. and T.V. MCEVILLY, 1974, Near-field observations and source parameters of central California earthquakes, *Bull. Seism. Soc. Am.*, **64**, 1855-1886.
- KARAKAMA, I., I. OGINO, K. KANJO, K. TSUMURA, M. TAKAHASHI and R. SEGAWA, 1980, The earthquake swarm east off the Izu Peninsula of 1980, *Abstract, Annual Meeting Seism. Soc. Japan*, No. 2, p. 3 (in Japanese).
- MADARIAGA, R., 1976, The dynamics of an expanding circular fault, *Bull. Seism. Soc. Am.*, **66**, 639-666.
- MOGI, K., 1963, Some discussion on aftershocks, foreshocks and earthquake swarms—the fracture of a semi-infinite body caused by an inner stress origin and its relation to the earthquake phenomena (third paper), *Bull. Earthq. Res. Inst.*, **41**, 615-658.
- RAUTIAN, T.G. and V.I. KHALTURIN, 1978, The use of coda for determination of the earthquake source spectrum, *Bull. Seism. Soc. Am.*, **68**, 923-948.
- TERASHIMA, T., 1968, Magnitude of microearthquake and the spectra of microearthquake waves, *Bull. Internat. Inst. Seism. and Earthq. Eng.*, **5**, 31-108.
- THATCHER, W. and T.C. HANKS, 1973, Source parameters of southern California earthquakes, *J. Geophys. Res.*, **78**, 8547-8576.
- TSUJIURA, M., 1973, Spectrum of seismic waves and its dependence on magnitude (1), *J. Phys. Earth*, **21**, 373-391.
- TSUJIURA, M., 1978a, Spectral analysis of the coda waves from local earthquakes, *Bull. Earthq. Res. Inst.*, **53**, 1-48.
- TSUJIURA, M., 1978b, Spectral analysis of seismic waves for a sequence of foreshocks, main shock and aftershocks: the Izu-Oshima-kinkai earthquake of 1978, *Bull. Earthq. Res. Inst.*, **53**, 741-759 (in Japanese).
- TSUJIURA, M., 1979a, Mechanism of the earthquake swarm activity in the Kawanazaki-oki, Izu Peninsula, as inferred from the analysis of seismic waveforms, *Bull. Earthq. Res. Inst.*, **54**, 441-462.
- TSUJIURA, M., 1979b, The difference between foreshocks and earthquake swarm, as inferred from the similarity of seismic waveform (preliminary report), *Bull. Earthq. Res. Inst.*, **54**, 309-315 (in Japanese).
- TSUJIURA, M., 1980a, Earthquake swarm activity in the northern Tokyo Bay, *Bull. Earthq. Res. Inst.*, **55**, 601-619.
- TSUJIURA, M., 1980b, Activity mode of the earthquake swarm (4), a prediction of the largest earthquake, *Abstract, Annual Meeting Seism. Soc. Japan*, No. 2, p. 81 (in Japanese).
-

## 1. 1980年伊豆半島東方沖の群発地震の活動様式

地震研究所 辻 浦 賢

1980年6月24日頃より7月末にかけ、伊豆半島東方沖で最大  $M 6.7$  を含む顕著な群発地震が発生した。前回の群発地震(1978年, 11月—12月)に続き、今回の群発地震についても、活動の活発な時間帯を選び、それらの地震についての波形並びにスペクトル解析から、その活動様式についていくつかの特徴ある結果を得た。主な結果は次の通りである。

(1) 震源域を囲む5個所のテレメーター観測所の早送り記録(25 mm/sec)の重ね合わせにより波形について調べた結果、ある限られた時間帯(例えば15分)に発生する地震は、 $S-P$  時間を含め非常に似かよった波形を示し、所謂“相似地震”の集合(Earthquake family)であることが解った。この様な傾向は5個所の観測所すべてについて共通である。

(2) 一連の相似地震の活動が終ると震源域の移動がみられ、別の相似地震群が得られる。更に活動の継続と共に別の震源域へ移動し、約1時間続いた活動から4種類の相似地震群が得られた。但し、 $M 6.7$  を持つ最大地震、並びにその直後の地震の活動様式は本震—余震型を示し、相似地震は現われない。

(3)  $S$  波についてのスペクトル解析から、相似地震の Corner frequency は  $M=2.0-4.6$  の間で略一定であり、その値はその地震群に含まれる最大地震の大きさに依存する。

集中した活動をもつ時間帯11組の地震について調べた結果、 $M 6.7$  の地震系列を除き、約80%のものがいずれかの組に属する相似地震であることが解った。(1), (2), (3)の結果からみて、夫々の相似地震は、ある限られたせまい範囲(数百米)、おそらく同じ断層面上で繰返し発生したことが推定される。